Solid Freeform Fabrication 2016: Proceedings of the 27th Annual International Solid Freeform Fabrication Symposium – An Additive Manufacturing Conference
Reviewed Paper

Selective Separation Sintering for Metallic Part Fabrication

Behrokh Khoshnevis, Jing Zhang

University of Southern California, Department of Industrial and Systems Engineering

Los Angeles, CA, 90007

Abstract

Selective Separation Sintering (SSS) is a powder layer based additive manufacturing approach. In the printing process a dry powder of higher sintering temperature is deposited into the base material which makes up the part. The inserted powder defines the boundary of the part and separates the part from its surroundings. A post sintering of the part is carried out in the furnace where the base material is sintered and the inserted powder remain loose due to its higher sintering temperature. The part is separated from the surrounding redundant material along the loose inserted powder region. A stable deposition rate of S-powder is the key for generating parts of easy separation and smooth surface. Factors that affect the flow rate are analyzed and the analyzed results are implemented to stabilize the process. With the progress in powder deposition rate control, bronze parts have been fabricated which demonstrate good quality.

Key words: Selective separation sintering (SSS), sintering, powder deposition, additive manufacturing

1. Introduction

The commercially available (AM) additive manufacturing technologies for fabricating metallic parts employ high power density beams or apply binder with post sintering. To date, selective laser/electron beam melting (SLM & EBM) are most often used AM methods to produce near full density metallic parts of high resolution. Due to high up-front investment (~$1 million) and expensive operating and maintenance cost, SLM and EBM are mainly used by big corporations or institutes like NASA, GE, hospitals and universities. In cases where full density is not required or infiltration is acceptable, a relatively low cost approach like sintering is more appropriate. Selective laser sintering (SLS) has similar hardware and operating environment requirements as that of SLM which makes SLS also a high cost approach [1]. Green parts bonded by binder with post sintering by ExOne is capable of manufacturing metallic parts at relatively low cost but the binder also contaminates the parts [2]. The binder approach has problems to process materials sensitive to contamination such as titanium alloys [3]. Selective inhibition sintering (SIS) takes an opposite of ExOne binder approach by inhibiting the boundary of the part during sintering, providing an economic solution for making certain metals, including bronze. The applicability of SIS in more metallic materials is still under investigation [4].

There are few commercially available technologies that can produce functional ceramic parts. Electron beam melting cannot be applied to ceramics due to the fact that most ceramics are electrically non-conductive. Laser beam melting of ceramics faces the problem of cracks formation as a result of large thermal stress [5]. Efforts to preheat the powder bed to high temperature (e.g. 1600 °C) can avoid cracks formation but long time preheating may cause rough edge due to solid phase sintering of non-part powder [6]. Binder based technologies (including Stereolithography based approach) do not have the problem of cracks formation during printing. While in the pyrolysis stage, the space previously occupied by the binder is released and large shrinkage rate is to be expected [7].

Under such context, SSS (Selective Separation Sintering) is developed to print functional parts at relatively low cost with high quality for a variety of materials including ceramics [8], metals, etc.

1.1. Operating Principles of SSS

In the SSS process, two kinds of powders are used, the base powder (B-powder), which makes up the final part, and the separator powder (S-powder) which isolates the part from the surrounding B-powder region. The S-powder is selectively deposited into the B-powder layer, forming a barrier surrounding the loose powder that eventually becomes the part. The printed green part is moved into a furnace for bulk sintering. After sintering, the S-powder coating remains loose and unsintered, making the part easily removable.

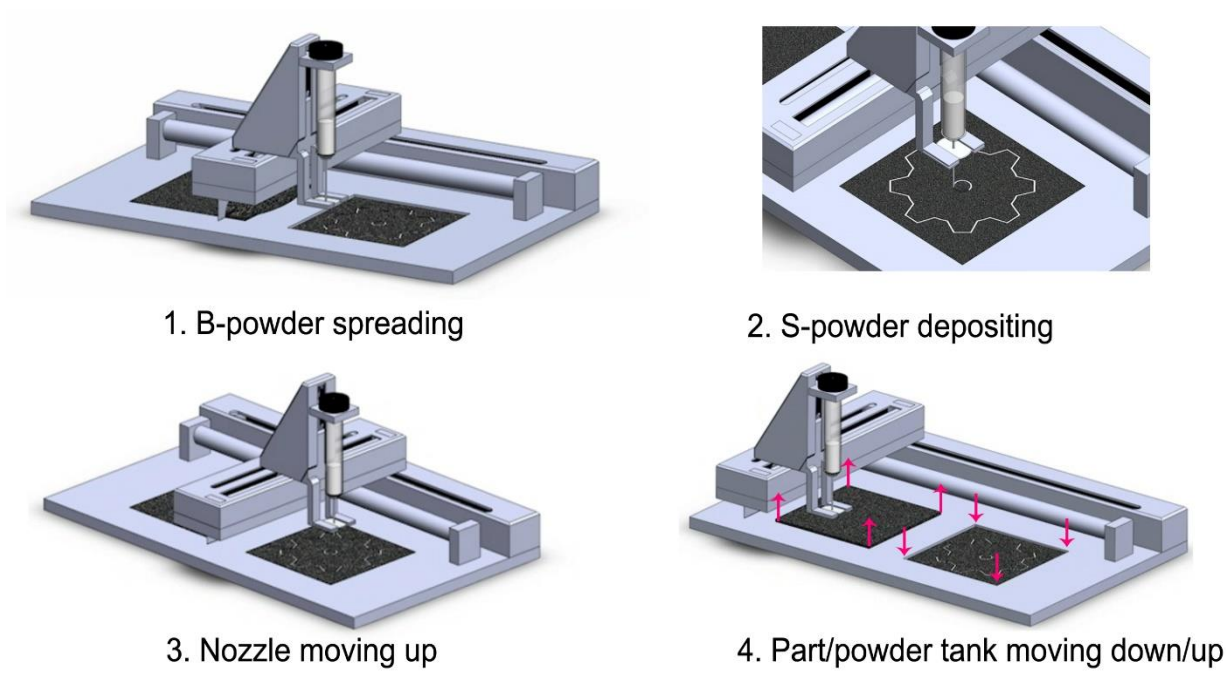

Figure 1. Printing process of SSS. 1. B-powder spread; 2. S-powder deposition; 3. Nozzle raised; 4. Part tank lowered, powder tank raised (Photo Courtesy: Brian Chantrupon)

The SSS process can be described by the following steps as illustrated in Figure 1:

1. A thin layer of B-powder is spread over the part tank;
2. The S-powder deposition nozzle is lowered into the B-powder layer, selectively depositing the S-powder at the layer boundary;
3. The nozzle is raised to provide clearance for subsequent movement;
4. Raise up the B-powder storage tank and lower the platform for one-layer thickness;
5. Steps 1-4 are repeated until all layers are completed;
6. The green part is moved to a sintering furnace.
7. The sintered part is removed from the furnace. The surrounding material is easily removed revealing the final part.

The S-powder is delivered inside the base powder by means of a thin conduit at the end of nozzle made of a narrow hollow needle (such as a hypodermic needle shown in Figure 2 (a).

Normally, granular materials form an arch in a tight conduit [8-10], as shown in Figure 2 (b). However, with the addition of vibration through a piezo electric element, a controlled and continuous flow of powder can be achieved as illustrated in Figure 2 (c). Vibrating the conduit agitates the particles touching the inner wall of the conduit and results in the breaking of the bridge and hence flows of the S-powders. When vibration stops an arch pattern quickly returns and stops the flow.

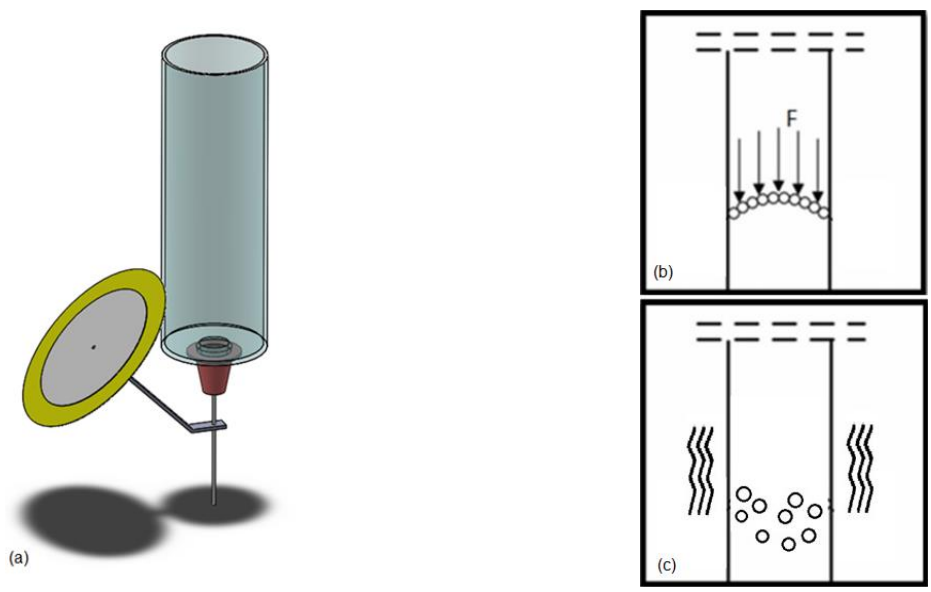

Figure 2 The dry powder delivery system. (a): The S-powder deposition system. (b) The arch pattern the stops powder flow (c) The arch pattern broken by vibration

Successful separation of the part is dependent on the difference in sintering temperature between the S-powder and the B-powder. As illustrated in Figure 3, the green piece in the furnace is heated up following a chosen sintering profile. The actual sintering temperature (blue) is chosen by experiments that it is higher than the sintering temperature of B-powder (green), but not high enough to sinter the S-powder (red). As a result, the B-powder becomes well sintered, while the S-powder remains loose.

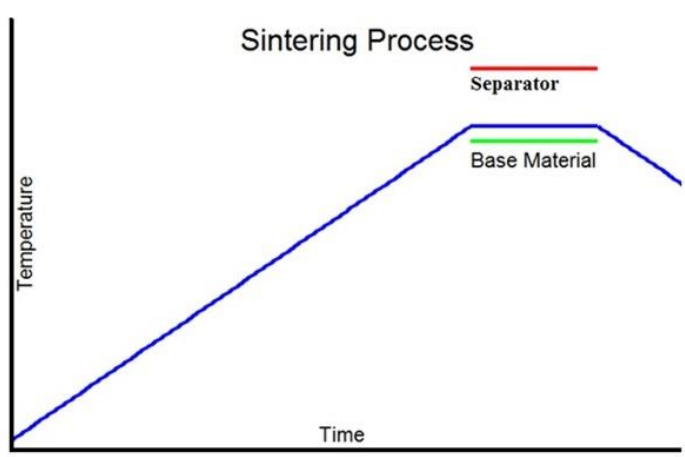

Figure 3. Sintering process for SSS. Blue: heating ramp; red: sintering temperature of S-powder; green: sintering temperature of B-powder.

An illusion of separation sintering is provided in Figure 4. The black spheres represent the B-powder and the white spheres represent the S-

powder. Figure 4 (a) illustrates the S-powder wall after deposition into the B-powder layer. In the course of sintering, the B-powder particles only fuse with the neighboring B-powder particles to form a solid piece while the S-powder regions remain loose. The part is then separated with ease by removing the loose S-powder.

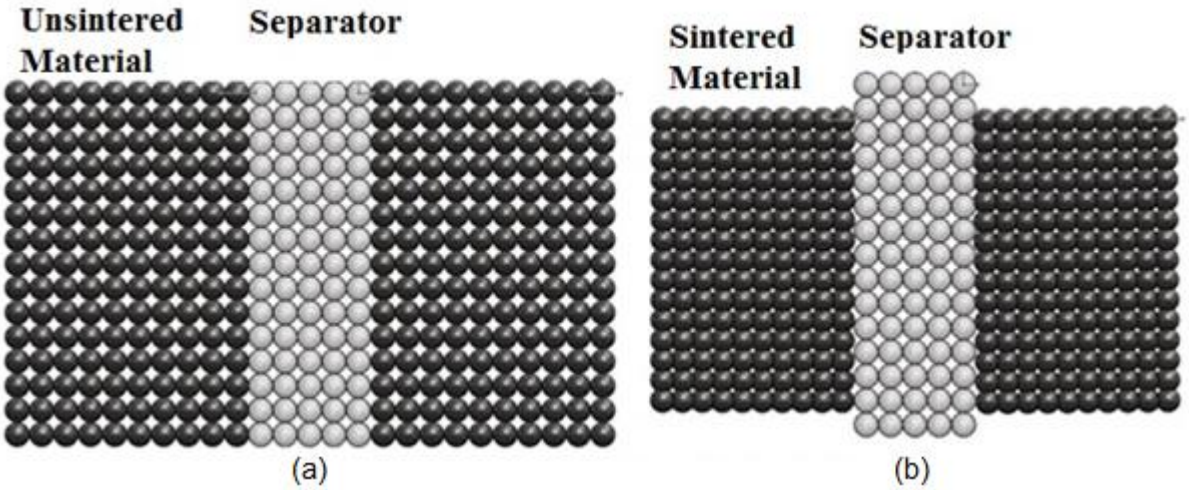

Figure 4. Illustration for SSS principle (a) before sintering; (b) after sintering – B-material shrinks while S-material does not. (The black spheres represent the building material and the white spheres represent the separator)

1.2. Previous experimental results

SSS has been applied in producing ceramic and metallic parts under the support of NASA for creation of Lunar landing pads using in-situ materials [11]. The ceramic material was lunar regolith simulant labeled JSC-1A[1] and was sifted to be under 200 μm. Sintering was carried out in ambient environment in a muffle furnace. The sintered interlocking tiles may be patterned in-place and sintered by microwave for creation of planetary landing pads as shown in Figure 5.

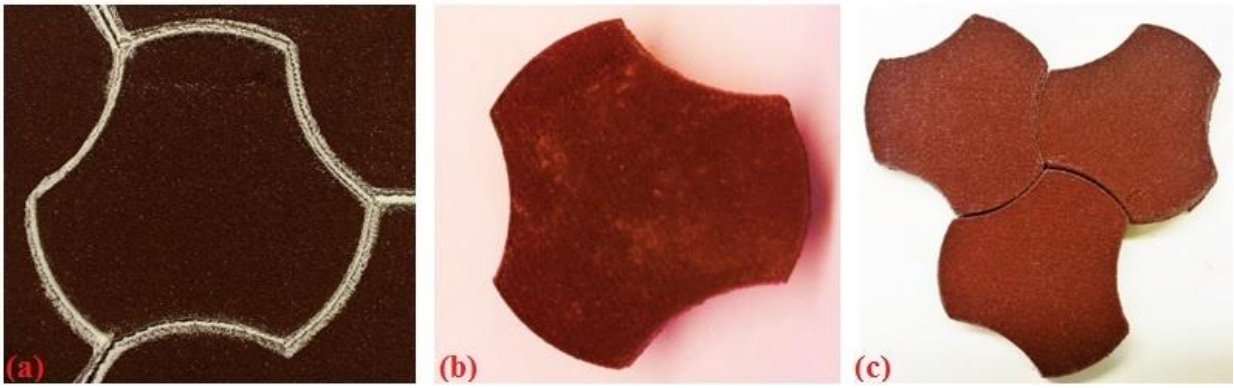

Figure 5. The sintered ceramic pieces of JSC-1A. (a) The sintered brick unit after sintering; (b) The separated brick unit; (c) Interlocking tile pattern

[1] Purchased from www.orbitec.com

Bronze and steel powder material have been tested [12]. Both powders have a mesh size of 325 and are sintered to their correspondingly profiles. As can be observed from Figure 6 (a), there is one dark line in the perimeter of the half cone. The intentional missed deposition of one layer of S-powder caused the part to connect with its surrounding at the missing circle and yielded that defect.

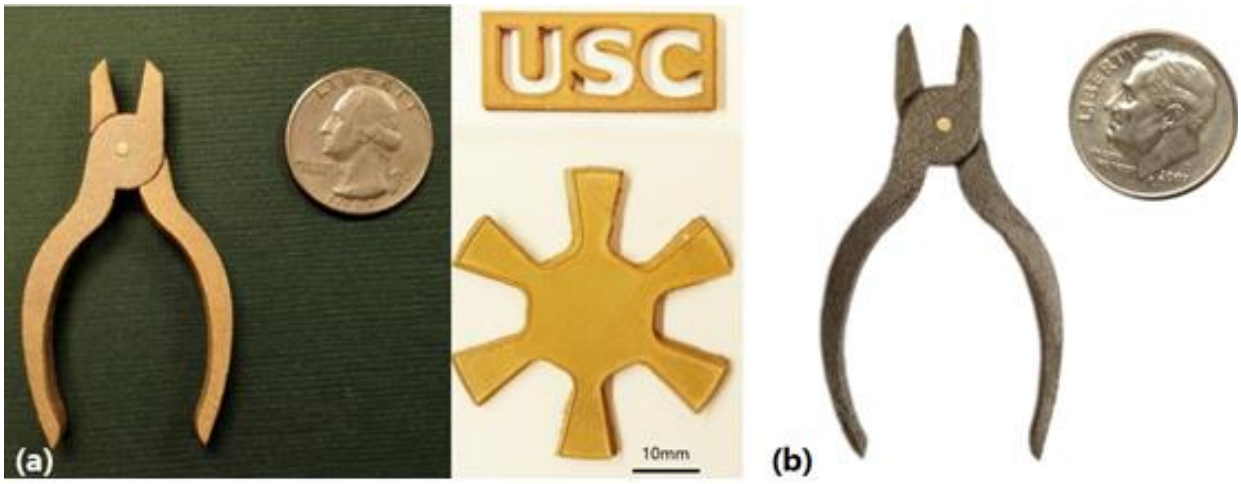

Figure 6. Metallic samples by SSS (a) Bronze (b) Steel parts

In SSS, powder deposition flow rate determines the ease of separation and dominates the surface quality. Therefore, identification of significant factors for deposition rate is of great interest in the process. Research has been carried out to determine the factors responsible for flow rate and stability, including nozzle size, waveform shapes and frequency.

2. Study on significant factors to achieve stable S-powder deposition rate

A powder confined in a thin conduit can be activated for free flow under vibration. The flow rate has been observed to respond to conduit size, vibration frequency, etc. To understand the factor of importance for controlling the flow rate, deposition experiments have been carried out.

2.1. Initial experiments to identify dominant factors

The factors under study include: powder species, inner diameter of the conduit, wave shape and frequency. As the powder deposition rate shows an increase with the increased amplitude before the piezo disc breakdown, the amplitude is kept constant below the breakdown voltage. The powder species include the powder size, shape, material and etc. which determine the intrinsic flowability of the powder. Bronze powder was chosen for testing (grade: 5807C from Accu powder). A full factorial design at 3 levels is applied to this set of experiments which correspond to 27 trials. The details of the factors and levels of each are represented in the table below:

Table 1. Levels of the Full Factorial Design

	Level		
Factors	0	1	2
A: Needle size/μm	L	M	S
B: Wave Shape	Square	PS	NS
C: Frequency	L	M	H

Using R to analyze the data and an ANOVA table is generated as shown:

From the ANOVA result shown in Figure 7 it can be seen that at a confidence level of 95%, the factor of the conduit size is the only factor of importance. Such a conclusion does not agree with the prior observations which indicate that the flow rate changes with frequency. The suspected cause of this discrepancy may be some large noise that masks out crucial information.

```
Analysis of Variance Table

Response: Flowrate
          Df Sum Sq Mean Sq F value Pr(>F)
A          2 1.3631 0.68154  3.7987 0.0286 *
B          2 0.6512 0.32560  1.8148 0.1727
C          2 0.7440 0.37198  2.0733 0.1357
AB         2 0.0442 0.02209  0.1231 0.8844
AB2        2 0.0778 0.03888  0.2167 0.8059
AC         2 0.3673 0.18365  1.0236 0.3662
AC2        2 0.1733 0.08665  0.4830 0.6196
BC         2 0.0384 0.01918  0.1069 0.8988
BC2        2 0.1007 0.05037  0.2808 0.7563
ABC        2 0.0081 0.00404  0.0225 0.9777
ABC2       2 0.0721 0.03605  0.2009 0.8186
AB2C       2 0.2157 0.10783  0.6010 0.5519
AB2C2      2 0.1906 0.09531  0.5312 0.5909
Residuals 54 9.6882 0.17941
```

Figure 7. ANOVA analysis for factors of importance

To further study these phenomena and reduce the noise among different runs, the deposition rate against running order is plotted. It is observed that the deposition rate decreases with the increased running orders as illustrated in Figure 8. Generally, it can be seen that flow rates quickly descend to a low flow rate from an initially large value. The red plot in the 3rd replicate have all the powder refilled after the previous run and it yields a much larger value. Considering that powder compacts by vibration each time as the experiments continue, it is hypothesized that the damping effect in the flow rate is due to compaction.

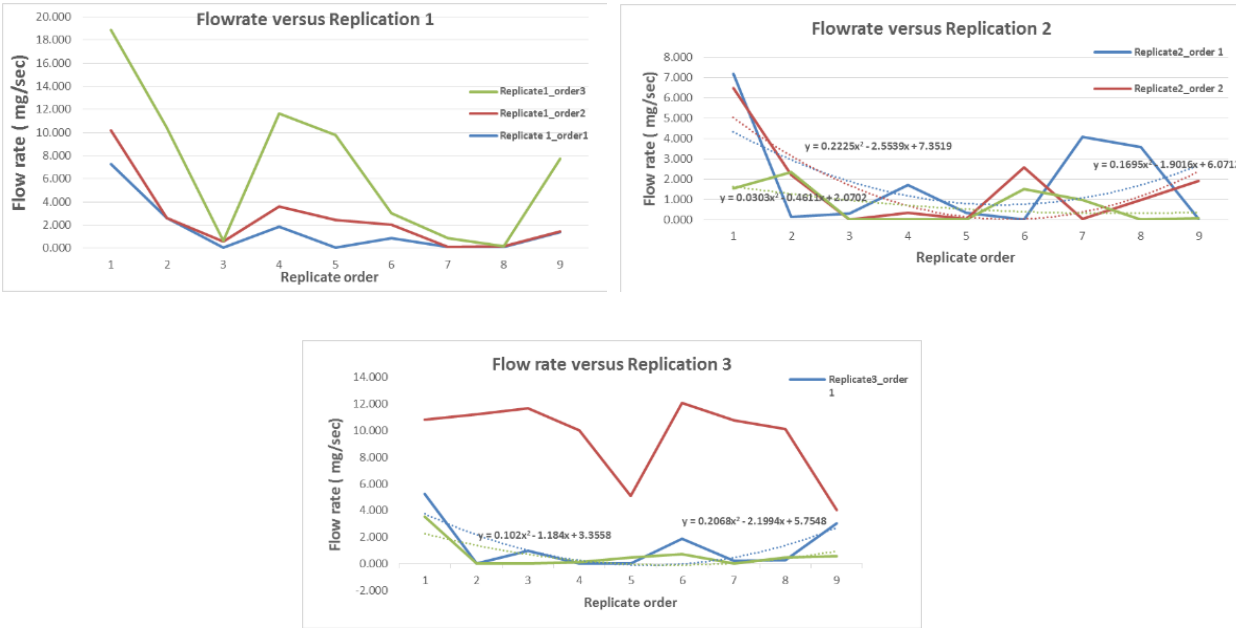

Figure 8 Plot of deposition rate against running order for all replicates

2.2. Study on the role of compaction

As the powder flow rate may be affected by the compaction of powder, experiments are carried out to study the compaction effect on the powder flow. The experimental setup is as shown in Figure 9. A glass syringe is used to store the powder (the same 5807C bronze powder is used). The piezo disc is put under the powder as in the case of the SSS machine setup. The opening of the conduit is sealed. Vibration is turned on to compact the powder and the height of the powder is measured. A control experiment where the same amount of powder filled in the syringe is allowed to deposit the powder and the deposited powder weight is measured.

These experiments show that the powder flow rate decreases with the increased compaction rate. As shown in Figure 9 (b) the height of the powder inside the syringe reduces rapidly in the beginning and stabilizes at about 88% of its original height. The quick compaction rate in the beginning is also reflected in the powder deposition rate as in Figure 9 (c), which has almost the same shape as that of the compaction curve. A stable flow rate is eventually achieved as a stabilized compaction rate is reached.

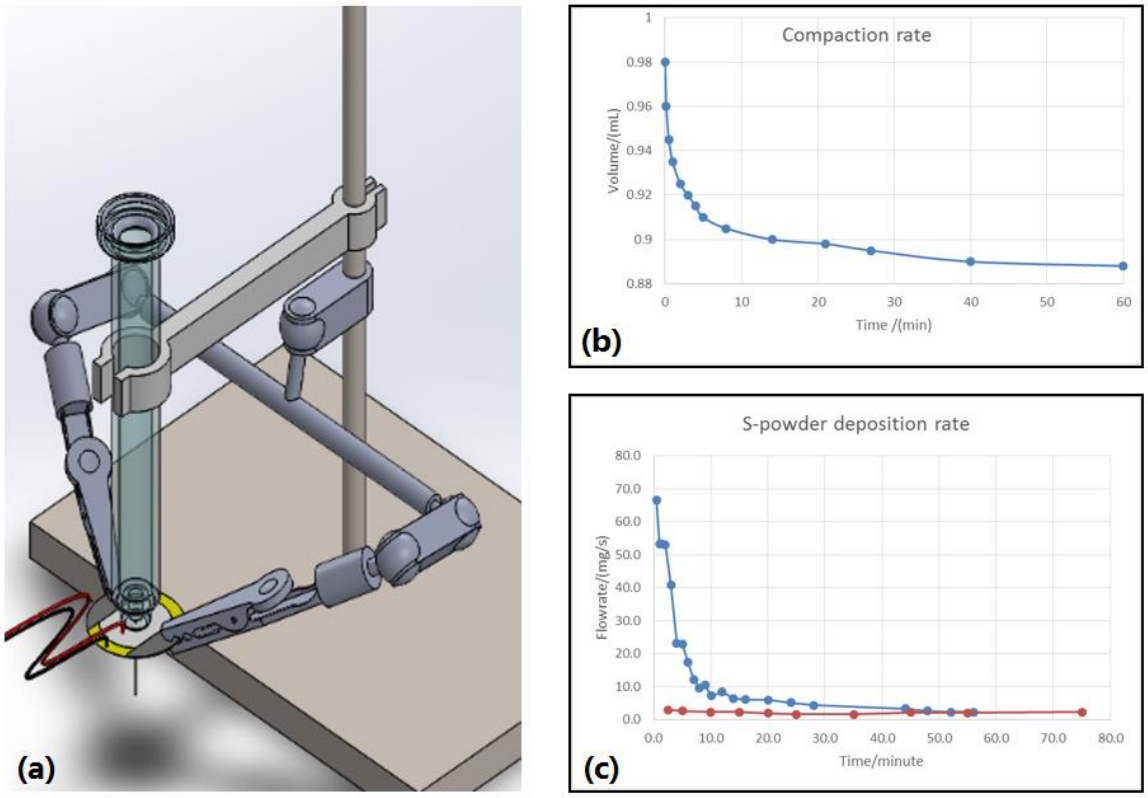

Figure 9. Experimental setup for compaction study (a) Experiment setup (b) Measured height of S-powder over time (c) the correlated S-powder flow rate. The red line represents the stabilized flow rate after 45 minutes of vibrational compaction.

As the influence of compaction is critical to the powder deposition rate, a changing compaction rate will therefore rule over signals such as frequencies and wave shapes. Such a challenge maybe overcome with continuous feeding of S-powder into the powder reservoir, i.e., the syringe shown in Figure 2. By retaining less powder inside the syringe, the S-powder in the syringe is discharged before it is compacted. The powder deposition rate is controlled by the movement of the nozzle because the S-powder can only flow out into the B-powder when the nozzle makes space for it.

3. Experimental results with proper control over compaction rate

The research work illustrates that with a more stable compaction rate, the deposition rate can remain high and the printed parts have better consistency over the surface quality.

Spherical tungsten powder is used as the S-powder in the following experiments and the bronze powder used is AccuPowder 5807C of 325 meshes. A bearing house is made to hold a bearing tightly as designed as shown in Figure 10.

Figure 10. Bronze bearing housing

4. Analysis

Both standalone test and the printing test verify that a stable powder deposition rate may be achieved. Continuous feeding of S-powder into the powder reservoir helps to reduce the compaction rate and increases the stability of S-powder deposition. The printed parts with smooth surface also support this evidence. Future research will include automatic mechanism for controlling the compaction rate and understanding other factors of importance.

5. Summary

SSS, developed to bring down the cost of additive manufacturing of metals and ceramics, has been proven effective and efficient through fabrication of a variety of samples. The approach is also expected to work with all the metals and ceramics that may be sintered, regardless of how high the sintering temperature may be. The impact of powder compaction over powder deposition rate is observed and understood. A continuous feeding of S-powder is applied to maintain a stable powder deposition rate. The experiments have demonstrated the feasibility, ease and quality of the process with respect to accuracy, surface finish and density of the parts produced.

6. Acknowledgement

The research reported here has been supported by the National Science Foundation Grant CNMI No. 1131271 and NASA Innovative Advanced Concepts Grant No. NNX12AQ57G.

7. References

[1] M Agarwala, D Bourell, J Beaman, H Marcus, J Barlow. Direct selective laser sintering of metals, Rapid Prototyping Journal. 1 (1995) 26-36.

[2] Y Bai, CB Williams. An exploration of binder jetting of copper, Rapid Prototyping Journal. 21 (2015) 177-185.

[3] G Wen, P Cao, B Gabbitas, D Zhang, N Edmonds. Development and design of binder systems for titanium metal injection molding: An overview, Metallurgical and Materials Transactions A. 44 (2013) 1530-1547.

[4] P Torabi, M Petros, B Khoshnevis. Enhancing the resolution of selective inhibition sintering (sis) for metallic part fabrication, Rapid Prototyping Journal. 21 (2015) 186-192.

[5] RS Khmyrov, SN Grigoriev, AA Okunkova, AV Gusarov. On the Possibility of Selective Laser Melting of Quartz Glass, Physics Procedia. 56 (2014) 345-356.

[6] H Yves-Christian, W Jan, M Wilhelm, W Konrad, P Reinhart. Net shaped high performance oxide ceramic parts by selective laser melting, Physics Procedia. 5, Part B (2010) 587-594.

[7] X Song, Y Chen, TW Lee, S Wu, L Cheng. Ceramic fabrication using Mask-Image-Projection-based Stereolithography integrated with tape-casting, Journal of Manufacturing Processes. 20 (2015) 456-464.

[8] G Enstad. On the theory of arching in mass flow hoppers, Chemical Engineering Science. 30 (1975) 1273-1283.

[9] S Yang, JRG Evans. Acoustic control of powder dispensing in open tubes, Powder Technol. 139 (2004) 55-60.

[10] DM Walker. An approximate theory for pressures and arching in hoppers, Chemical Engineering Science. 21 (1966) 975-997.

[11] B Khoshnevis, J Zhang, Selective Separation Sintering (SSS)-An Additive Manufacturing Approach for Fabrication of Ceramic and Metallic Parts with Applications in Planetary Construction, AIAA SPACE 2015 Conference and Exposition. 2015.

[12] J Zhang, B Khoshnevis, Selective Separation Sintering (SSS) A New Layer Based Additive Manufacturing Approach for Metals and Ceramics, Solid Freeform Fabrication Symposium 2015 (2015).